Technobius Physics, 2024, 2(2), 0013, https://doi.org/10.54355/tbusphys/2.2.2024.0013

Technobius Physics

https://technobiusphysics.kz/

e-ISSN 3007-0147

Corrigendum Notice: A corrigendum has been issued for this article and is included at the end of this document.

Article

Comprehensive analysis of solar cell behavior: effects of light intensity, temperature, and operational modes

Ersaiyn Bekbolsynov*

Faculty of Physics and Mathematics, Bukhara State University, 11 Mukhammad Iqbol st., Bukhara, Uzbekistan
*Correspondence: ersaiynb@mail.ru

Abstract. This study investigates the current-voltage characteristics of a solar cell under varying light intensities, temperatures, and operational conditions to comprehensively assess its performance. The experimental approach involves measuring short-circuit current and open-circuit voltage at different light intensities and constructing current-voltage curves to analyze the solar cell's response to changing illumination levels. The dependence of open-circuit voltage and short-circuit current on temperature is also estimated to understand thermal influences on the solar cell's electrical properties. Additionally, the solar cell's behavior is examined under different operational modes, including cooling with a blower, operation without cooling, and light filtration through a glass plate. The corresponding current-voltage characteristics are plotted to evaluate the impact of thermal management and light modulation on the solar cell's efficiency and stability. Furthermore, the characteristic curve of the solar cell is determined under natural sunlight illumination to simulate real-world conditions. The findings provide valuable insights into optimizing solar cell performance for practical applications and sustainable energy systems. This research contributes to advancing our understanding of solar cell behavior under diverse environmental and operational settings, with implications for enhancing solar energy utilization and promoting renewable energy technologies. Future studies will focus on refining solar cell design and operation based on these insights to maximize efficiency and reliability in solar power generation.

Keywords: solar cell, current-voltage characteristics, light intensity, temperature dependence, operational modes, thermal management, renewable energy, sustainability.

1. Introduction

Silicon, a fundamental element in the periodic table with the atomic number 14, is widely recognized for its importance in modern technology, particularly in the semiconductor industry. Pure silicon, when isolated and characterized, displays several unique properties essential for its applications in electronics and various scientific endeavors [1]. Pure silicon primarily exists in a crystalline form with a diamond cubic crystal structure. Each silicon atom is covalently bonded to four neighboring silicon atoms, forming a stable and rigid lattice. This crystal structure contributes to silicon's robustness and resilience under varying environmental conditions [2].

One of the most notable properties of silicon is its semiconductor nature [3]. Silicon's electronic properties are influenced by its four valence electrons [4]. At absolute zero temperature, silicon behaves as an insulator due to the completely filled valence band and an empty conduction band. However, at higher temperatures or under specific conditions, silicon can become a semiconductor by promoting electrons from the valence band to the conduction band, thereby facilitating electron mobility crucial for electronic conductivity [5].

To create a $p-$ or $n-$ type semiconductor, pure silicon is purposefully "impurified" (doped) with triand pentavalent impurity atoms [6]. The junction formed when $p-$ and $n-$ type crystals are combined determines the solar cell's electrical characteristics (Figure 1). When there is no external voltage present and the system is in equilibrium, the Fermi characteristic energy level remains

constant. Electrons diffuse into the $p-$ region and holes into the $n-$ region due to the differences in the concentrations of electrons and holes in the two regions. A space charge-limited current area is formed by the immobile impurity atoms, and the diffusion current and the field current balance each other out in an equilibrium [7–9].

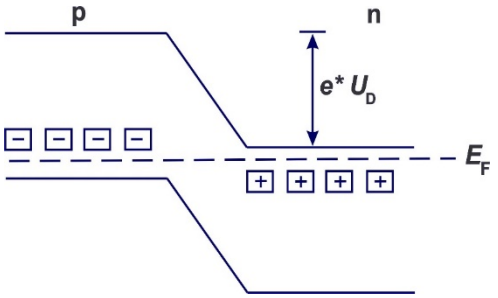

Figure 1 – The energy-band scheme's + donors and – acceptors are located at the pn – junction, where e represents the elemental charge and U_D is the diffusion potential

The initial disparity in Fermi energy levels between the separate $p-$ and $n-$ regions is indicated by the diffusion potential U_D in the pn – junction, and this is contingent upon the doping level. In silicon under typical conditions, the gap between the valence and conduction bands is fixed $E = 1.1\ eV$. The diffusion potential of silicon is between 0.5 and 0.7 eV. The detail construction on Figure 2.

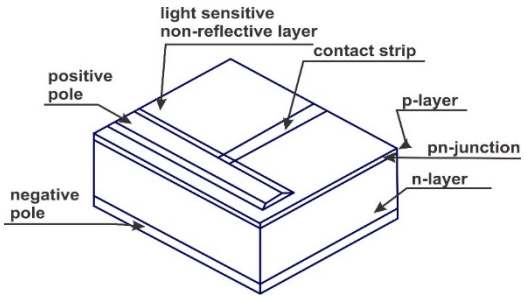

Figure 2 – Putting together a silicon solar cell

Photons from light striking the $pn-$ junction form electron-hole pairs that are divided by the space charge [10-11]. The $n-$ region absorbs electrons, while the $p-$ region absorbs holes. In addition to the $pn-$ junction, the $p-$ layer above it also absorbs photons. The generated electrons are minority carriers in those regions because recombination significantly lowers their concentration and, consequently, their efficiency. In order for the electrons of diffusion length l_e to enter the $n-$ layer, the $p-$ layer needs to be thin enough: $L_E \gg t$, in a view of the t is the $p-$layer's thickness.

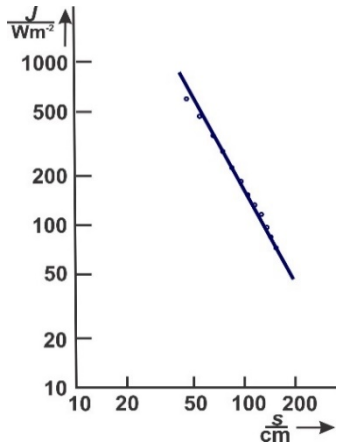

Figure 3 – Intensity of the light at standard distances from the source

When a voltage U is placed across the $pn-$ junction and g, the number of electron-hole pairs generated per unit area, a stream of electrons and holes with a density is formed:

$$i = e * \left(e^{\frac{eU}{kT-1}}\right) * \left(\frac{n_0 D_e t}{L^2 e} + \frac{p_0 D_h}{L_h}\right) - eg \quad (1)$$

When: e – the elementary charge; k – Boltzmann's constant; T – the temperature; L – the diffusion length of electrons and holes; D – the diffusion constant for electrons and holes; n_0 and p_0 are equilibrium concentrations of the minority carriers.

At a constant temperature, the short-circuit current density $(U = 0)$ $i_s = -e * g$ is proportional to the incident light's intensity. The temperature increases with g becoming very slightly greater, less than $10^{-2}\ \frac{\%}{K}$. The voltage U is limited to reaching the same height as the diffusion potential U_D. The no-load voltage normally drops by $-2.3\frac{mV}{K}$ as the temperature rises because the equilibrium concentrations n_0 and p_0 rise with temperature:

$$n_0 \sim e^{-\frac{\Delta E}{2kT}} \quad (2)$$

This research aims to study a solar cell's current-voltage properties at various light intensities. Plot the current-voltage characteristic at various light intensities after measuring the short-circuit current and no-load voltage at various light intensities. Compared to Calculate how temperature affects the short-circuit current and no-load voltage. Additionally, we are interested in experimenting with various modes and plotting the current-voltage characteristic under various operating conditions, such as blower cooling, no cooling, and beaming light through a glass plate. The final step is to identify the characteristic curve under solar illumination.

2. Methods

The experimental setup was designed to investigate the effects of light intensity and temperature on photovoltaic performance. A quadruple solar array composed of photovoltaic cells was used to convert solar energy into electricity. These cells formed the core measurement element of the study. A Moll-type thermopile, which exploits the Seebeck effect to convert thermal energy into electrical signals, was included to assess light intensity and temperature-induced effects. This thermopile was chosen for its high sensitivity and narrow angular aperture (~20°), making it suitable for detecting direct radiation only [5].

The main light source was a 220 V / 120 W incandescent lamp mounted on a ceramic E27 base, integrated with a reflector, switch, and protective plug. To simulate varying light intensities, the distance between the lamp and the solar cell was altered using a calibrated 1000 mm meter scale. Measurements were taken at multiple distances to observe the response under different irradiance levels. To reduce ambient stray light, a black cloth was draped over the optical bench. The thermopile was placed at a fixed distance of 0.5 m from the lamp to align with its angular sensitivity, while the solar panel was positioned further away to avoid light concentration effects that could distort the results.

To record variations in light intensity, the thermopile output was connected to a signal amplifier operating at a fixed input voltage of 10 V. Signal measurements were taken using digital multimeters (UNI-T UT61E), capable of capturing voltage, current, resistance, capacitance, and frequency with high resolution. Strong, insulated 500 mm cables with a 32 A rating connected all components.

A blower (1800 W) was used to regulate temperature. It could produce hot or cold air, depending on the requirement. During thermal tests, hot air was blown over the solar panel while a thermometer (range: -10 °C to +110 °C) was used to record the temperature immediately in front of the panel. A cooling fan ensured that the solar panel's base temperature remained stable. To avoid mechanical damage to the fragile p-layer of the cells, direct contact was avoided during measurements.

Glass plates (150 × 100 × 4 mm) were used to test the influence of transmitted and reflected light on photovoltaic output. A 20 cm long black cardboard tube was installed in front of the solar cell to shield it from diffuse light during direct sunlight measurements. These tests allowed comparison between the short-circuit current under direct versus combined (direct + diffuse) solar illumination.

Mechanical support was provided by stainless steel rods, heavy-duty clamps, flexible holders, and tripods. These enabled precise alignment of components and structural integrity of the setup. Plate holders ensured the glass sheets remained stationary during optical transmission experiments. The experimental circuit for volt-amperometric characterization was assembled as shown in Figure 1, and both the open-circuit voltage and short-circuit current were recorded prior to the main tests.

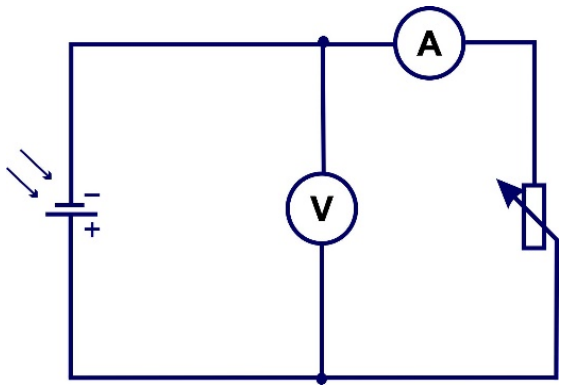

Figure 1 – Electrical circuit for measuring volt-apmetered characterization

All measurement data were logged and processed using Microsoft Excel for initial tabulation and plotting. OriginPro 2023 (OriginLab Corp.) was used for detailed data visualization, curve fitting, and statistical processing. For signal analysis and amplification calibration, LabVIEW software (NI) was used to automate and monitor input-output voltage readings across varying light and temperature conditions. To assess the relationship between short-circuit current (I_{SC}) and light intensity (E), linear regression was performed using the equation:

$$I_{SC} = \alpha E + b \quad (1)$$

Where α is the slope (representing current sensitivity per unit irradiance) and b is the offset. Temperature dependence of the open-circuit voltage (V_{OC}) was modeled using a second-order polynomial:

$$V_{OC}(T) = \alpha T^2 + \beta T + \Upsilon \quad (2)$$

Parameters α, β, and γ were determined by least squares fitting. Goodness-of-fit metrics such as the coefficient of determination (R^2) and root mean square error (RMSE) were used to evaluate fit quality. In addition, ANOVA was applied to compare the influence of cooling (fan vs. no fan) on power output, with significance set at $p < 0.05$.

3. Results and Discussion

For a more accurate and proper experiment, the short-circuit current and no-load voltage at different light intensities were first recorded. Figure 2 shows a plot of current versus voltage at different light intensities. Assume that the measuring surface receives all light that enters the 0.025 m diameter aperture. The graph illustrates a straight line on the graph representing the light intensity J dependence on distance s. One can calculate the light intensity at a distance of $s \leq 0.5$ m by extrapolating the straight line.

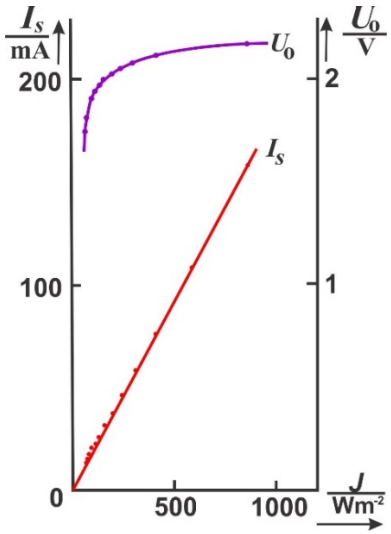

Figure 2 – The relationship between short circuit current and no-load voltage and light intensity

A solar cell with four series-connected cells that have a maximum no-load voltage of 2 V. The sensitivity of the measured equipment reached up to 0.16 mV/mW. Consequently, the intensity of light is described by the following level:

$$I_s = 1.84 * 10^{-4} \frac{A}{Wm^{-2}} * J \quad (3)$$

The values of volt-ampere characteristics were recorded at various light intensities and are displayed in Figure 3. The graph's dotted line connects the turning points of the curves, which represent the places at which the solar cell's internal resistance and the load resistor's values coincide to produce the greatest power production.

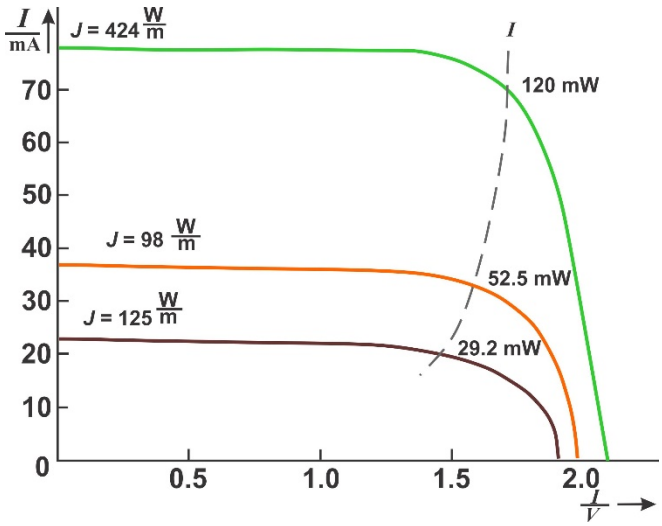

Figure 3 – Characteristics of current and voltage at various light intensities

As a result, as light intensity increases, internal resistance lowers. An efficiency of roughly 6% is obtained when the maximum output power and the incident power are compared, so solar panel area is 0.5 m^2.

The research has considered the impact of temperature as well as the distribution of temperature over the hot air area. The following equality was obtained by using hot and cold air to measure the no-load voltage:

$$\frac{\Delta U_0}{\Delta T} = -8 \frac{mV}{K} \quad (4)$$

It is important to remember that the measurements can only provide a rough order of magnitude. As a result, we get a value of $-2\ \frac{mV}{K}$ for a single cell. It is impossible to quantify how the short-circuit current changes with temperature.

For completeness of the experimental data, we additionally installed a glass plate, which is able to absorb light in the infrared region and hence used to reduce the temperature rise of the solar cell. Figure 4 is a graph showing the effect of the stack effect work from different 'modes of operation'. The graph shows three curves: the orange one refers to the fan-cooled mode; the green one indicates the fan-cooled mode; and the blue curve - when shielded with a glass plate. Note that the light intensity in the fan cooling mode is the maximum light intensity.

To identify the difference between different light sources, characteristic curves were recorded when illuminated by sunlight. Figure 5 shows a graph of the dependence of light intensity and wavelength, which shows curves from various sources. The spectral sensitivity of a silicon solar cell and the spectrum of the sun, which has a temperature of around 5800 K, and an incandescent bulb, which has a temperature of about 2000 K. Solar cells produce distinct properties when exposed to sunlight than incandescent lights do:

$$I_s = 3.04 * 10^{-4}\ \frac{JA}{Wm^{-2}} \tag{5}$$

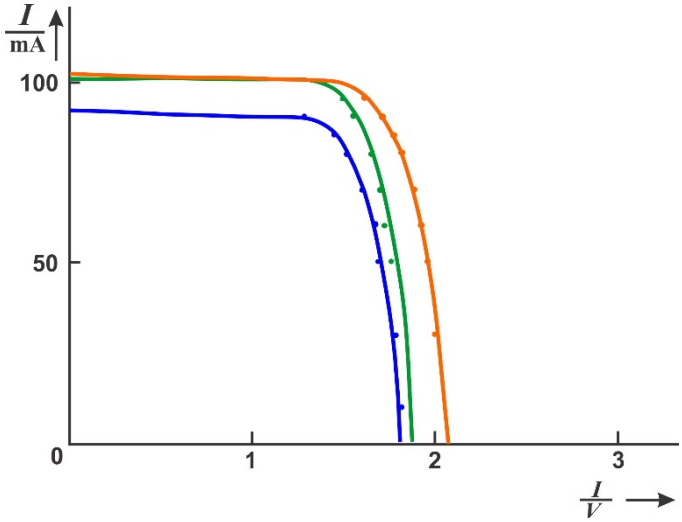

Figure 4 – Characteristics of the solar battery's current and voltage

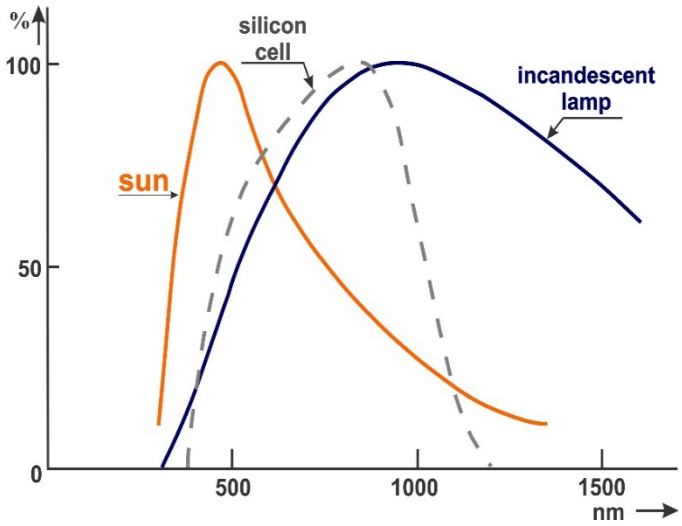

Figure 5 – Spectral characteristics of various sources

The two light sources' different spectra provide the explanation. Light from the sun produces a greater short-circuit current at the same intensity. The solar cell does not heat up as much in the

infrared part of the spectrum because of this, and measurements taken with and without cooling provide identical solar properties.

4. Conclusions

This investigation has provided valuable insights into the performance characteristics of a solar cell under varying light intensities, temperatures, and different operational conditions. Initially, the short-circuit current and open-circuit voltage were measured across a range of light intensities, allowing for the construction of current-voltage curves. These curves elucidated the impact of light intensity variations on the electrical output of the solar cell, crucial for understanding its efficiency under changing environmental conditions.

Subsequently, the study estimated the dependence of no-load voltage and short-circuit current on temperature. This analysis highlighted the influence of temperature fluctuations on the solar cell's electrical characteristics, offering insights into its behavior in practical applications.

Furthermore, the investigation evaluated the solar cell's performance under different operating modes, including cooling with a blower, operation without cooling, and light filtration through a glass plate. The corresponding I-V characteristics demonstrated the significance of thermal management and light modulation in optimizing the solar cell's efficiency and stability.

Moreover, the characteristic curve of the solar cell under natural sunlight illumination was determined. This final analysis provided practical data on the solar cell's behavior in real-world conditions, guiding future design and implementation strategies for solar energy systems.

In summary, the findings from this comprehensive study contribute to advancing our understanding of solar cell behavior under diverse environmental and operational settings. This knowledge is instrumental in improving the efficiency, reliability, and practicality of solar energy technologies, paving the way for sustainable and effective solar power generation systems. Continued research in this field will further refine our ability to harness solar energy for a cleaner and more sustainable future.

References

1. Stable Radicals: Fundamentals and Applied Aspects of Odd-Electron Compounds / K. Chandra Mondal, S. Roy, H. W. Roesky // Chemical Society Reviews. — 2016. — Vol. 45, No. 4. — P. 1080 - 1111. https://doi.org/10.1039/c5cs00739a
2. Space radiation applicability of pure silicon-core optical fibers / J. Xiao, Z. Hengjing, Zh. Hongqi, M. Xiping, J. Qiuyang // Infrared and Laser Engineering. — 2017. — Vol. 46, No. 8. — P. 822002. https://doi.org/10.3788/irla201746.0822002
3. The semiconductor silicon industry roadmap: Epochs driven by the dynamics between disruptive technologies and core competencies / S.T. Walsh, R.L. Boylan, C. McDermott, A. Paulson // Technological Forecasting and Social Change. — 2005. — Vol. 72, No. 2. — P. 213–236. https://doi.org/10.1016/S0040-1625(03)00066-0
4. Amorphous silicon enhanced metal-insulator-semiconductor contacts for silicon solar cells / S.L. Zhang, J. Shao, L.S. Hoi, S.N. Wu, B.F. Zhu, F. Shou-Shan, H.D. Li, D.P. Yu // Physica Status Solidi C: Conferences. — 2005. — Vol. 2., No. 8. — P. 3090–3095. https://doi.org/10.1002/pssc.200460765
5. Silicon-doped carbon semiconductor from rice husk char / S. Maiti, P. Banerjee, S. Purakayastha, B. Ghosh // Materials Chemistry and Physics. — 2008. — Vol. 109, No. 1. — P. 169–173. https://doi.org/10.1016/j.matchemphys.2007.11.011
6. Solid-state physics: Super silicon / R.J. Cava // Nature. — 2006. — Vol. 444, No. 7118. — P. 427–428. https://doi.org/10.1038/444427a
7. Carrier heating and its effects on the current-voltage relations of conventional and hot-carrier solar cells: A physical model incorporating energy transfer between carriers, photons, and phonons / C.-Y. Tsai // Solar Energy. — 2019. — Vol. 188. — P. 450–463. https://doi.org/10.1016/j.solener.2019.06.024
8. Electrical characteristics and hot carrier effects in quantum well solar cells / D.-T. Nguyen, L. Lombez, F. Gibelli, M. Paire, S. Boyer-Richard, O. Durand, J.-F. Guillemoles // Proceedings of SPIE - The International Society for Optical Engineering. — 2017. — Vol. 10099. — P. 127693. https://doi.org/10.1117/12.2251331
9. Direct measurement of the internal electron quasi-fermi level in dye sensitized solar cells using a titanium secondary electrode / K. Lobato, L.M. Peter, U. Würfel // Journal of Physical Chemistry B. — 2006. — Vol. 110, No. 33. — P. 16201–16204. https://doi.org/10.1021/jp063919z

10. The open-circuit voltage in microcrystalline silicon solar cells of different degrees of crystallinity / M. Nath, P. Roca i Cabarrocas, E.V. Johnson, A. Abramov, P. Chatterjee // Thin Solid Films. — 2008. — Vol. 516, No. 20. — P. 6974–6978. https://doi.org/10.1016/j.tsf.2007.12.052
11. Solar energy conversion with hot electrons from impact ionisation / P. Würfel // Solar Energy Materials and Solar Cells. — 1997. — Vol. 46, No. 1. — P. 43–52. https://doi.org/10.1016/S0927-0248(96)00092-X

Information about author:
Ersaiyn Bekbolsynov – Master Student, Faculty of Physics and Mathematics, Bukhara State University, 11 Mukhammad Iqbol st., Bukhara, Uzbekistan, ersaiynb@mail.ru

Author Contribution:
Ersaiyn Bekbolsynov – concept, methodology, resources, data collection, testing, modeling, analysis, visualization, interpretation, drafting, editing, funding acquisition.

Conflict of Interest: The authors declare no conflict of interest.

Use of Artificial Intelligence (AI): The authors declare that AI was not used.

Received: 09.03.2024
Revised: 25.04.2024
Accepted: 01.05.2024
Published: 03.05.2024

Technobius Physics, 2024, 2(2), 0013c, https://doi.org/10.54355/tbusphys/2.2.2024.0013c

Technobius Physics

https://technobiusphysics.kz/

e-ISSN 3007-0147

Corrigendum Notice: A corrigendum has been issued for this article and is included at the end of this document.

Post-Publication Notice

Corrigendum to “E. Bekbolsynov “Comprehensive analysis of solar cell behavior: effects of light intensity, temperature, and operational modes”, tbusphys, vol. 2, no. 2, p. 0013, May 2024. doi: 10.54355/tbusphys/2.2.2024.0013”

In the originally published version of this article, the Methods section lacked detailed information on experimental setup, instrumentation, and data processing procedures. The following corrections have been made:

1. Section 2 (Methods):

- The updated version now includes specific details on the experimental setup, measurement equipment (Moll-type thermopile, UNI-T UT61E multimeters), data logging tools (Microsoft Excel, OriginPro 2023, LabVIEW), and statistical analysis procedures (linear regression, polynomial fitting, ANOVA, RMSE evaluation).

- Additional clarifications were made regarding test conditions under different operational modes (blower cooling, no cooling, glass plate) and data reproducibility measures.

2. Figure 1 has been improved to enhance visual clarity of the experimental circuit schematic.

Additionally, the reference “Note on the properties of silicon / R. Hare // Journal of the Franklin Institute. — 1833. — Vol. 15, No. 6. — P. 362–363.” has been replaced with “Stable Radicals: Fundamentals and Applied Aspects of Odd-Electron Compounds / K. Chandra Mondal, S. Roy, H. W. Roesky // Chemical Society Reviews. — 2016. — Vol. 45, No. 4. — P. 1080-1111. https://doi.org/10.1039/c5cs00739a”.

These corrections do not affect the scientific results, discussion, or conclusions of the article but improve methodological transparency, reproducibility, and visual presentation.

Published: 20.05.2024